

# Investigation of surface integrity in high-speed ball end milling of cantilever shaped thin plate of Inconel 718

**N.N. Bhopale\*, R.S. Pawade**

Mechanical Engineering Department, Dr. Babasaheb Ambedkar Technological University, Lonere 402 103 Raigad, MS, India

\* Corresponding e-mail address: nandkumar.bhongle@sepracor.com

Received 18.10.2012; published in revised form 01.12.2012

## Manufacturing and processing

### ABSTRACT

The paper addresses the effects of cutting speed and feed on the work piece deflection and surface integrity during milling of cantilever shaped Inconel 718 plate under different cutter orientations. The experiments were conducted on a CNC vertical milling machine using 10 mm diameter TiAlN coated solid carbide ball end milling cutter. Surface integrity is assessed in terms of micro hardness beneath the machined surface. The micro-hardness profile shows different patterns at various cutting parameters. It is observed that at large cutting speed as well as feeds, thicker work piece with larger work piece inclination shows higher micro hardness as compared to the other machining conditions.

**Keywords:** Ball end milling; Cantilever; Surface integrity; Micro hardness; Inconel 718; Work piece deflection; Response surface methodology; Central composite design

#### Reference to this paper should be given in the following way:

N.N. Bhopale, R.S. Pawade, Investigation of surface integrity in high-speed ball end milling of cantilever shaped thin plate of Inconel 718, Journal of Achievements in Materials and Manufacturing Engineering 55/2 (2012) 616-622.

## 1. Introduction

The ball-end milling of thin-walled components is a widely used machining operation to generate three-dimensional complex profiles in aircraft and space shuttle industries. The superalloys are mostly used in the aerospace applications due to their ability to maintain excellent mechanical strength at elevated temperatures. The analysis of surface quality in a ball-end milling on inclined work pieces has been a topic of interest for several researchers. But the super alloy Inconel 718 is concerned none of the studies are reported in the literature. In order to explore the understanding of ball end milling of cantilever work pieces, the studies on similar materials are presented here. Lee et al. [1] performed ball-end milling operation on the cantilevers inclined at

0°, 15° and 45° with various cutter orientations. The lower work piece deflection and the better surface finish were observed at work piece tilt angle of 45° with vertical outward cutter orientation. Ezugwu et al. [4] found that the optimal feed increases, width-of-cut and depth-of-cut increases, which results into higher surface roughness of the machined surfaces as increases. Guimu et al. [5] observed that increasing cutting speed can lower the work piece deformation. Also, the highest as well as the lowest feed rates result into the conditions leading to unstable machining vibrations. It results into poor surface finish in milling of thin specimens of titanium (TC4). Yoon et al. [3] observed that during machining of tubular that parts, the cutting tool deflection has more pronounced effect on the surface than the work piece

deflection. This is contrary to open-ended cantilever-type geometries, where the component of work piece deflection is remarkably higher. Monsour et al. [12] found that an increase in either feed or axial depth of cut increases the surface roughness, while an increase in the cutting speed decreases the surface roughness. Wang et al. [2] observed an increase in the surface roughness with an increase in the feed, concavity (concavity angle  $> 2.5^\circ$ ) and axial relief angle in a slot-end milling of Al2014-T6 under both dry and coolant based. The coolant-based cutting conditions.

In most of the above studies, the effect of cutter orientation and flexibility of work piece on the Work piece deflection and surface quality have been addressed independently. However, in the case of thin and flexible parts, it is necessary to control the effect of work piece deflection on the machined surface quality. Therefore, the objective of this paper is to understand the effect of machining parameters and cutting tool orientation on the machined surface and subsurface at the fixed end and free end of the cantilever-shaped thin Inconel-718 plate in ball end milling.

## 2. Experiment design

### 2.1. Response surface method

RSM were originally developed to analyse experimental data and to create empirical models of observed response values Box and Draper [13]. RSM is a collection of mathematical and statistical procedures, and is good for the modelling and analysis of problems in which the desired response is affected by several variables. In this study, the approximation of the mathematical model will be proposed using the fitted second-order polynomial regression model, which is called the quadratic model. The necessary data for building the response mode are generally collected by the experimental design [1-13]. In this study, the experimental design adopts the centred central composite design (CCD) in order to fit the quadratic model of the RSM. The factorial portion of CCD is a full factorial design with all combinations of the factors at two levels (high, +1.5 and low, -1.5). Further to determine the intermediate levels of the selected factors a parameter ' $\alpha$ ' were calculated and using a CCD rotatable design the levels of the input parameter were determined.

This type of design is commonly called the rotatable CCD. Selecting appropriate input parameters is a crucial task in design of experiment. In this work, the effect of independent machining parameters viz. cutting speed, feed, work piece thickness, work piece and cutter orientations on the micro harness is proposed. The optimum parametric settings have been achieved to minimize the surface roughness and work piece deflection using response surface methodology (RSM) in the framework of central composite design (CCD). (see Fig. 1)

### 2.2. Experimental procedure

The ball-end milling was performed on inclined cantilever-shaped workpieces along two paths, horizontal outward and

vertical upward, and at  $45^\circ$  and  $15^\circ$  workpiece inclination angles. In addition, tests were also performed on the flat horizontal ( $0^\circ$ ) workpieces to compare the results.

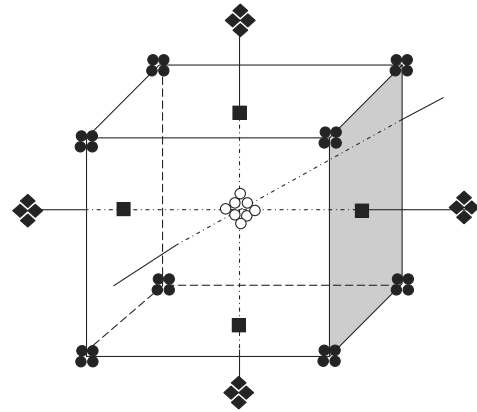


Fig. 1. Central composite design for four factors, where: ● - cube points, ◆ - axial points, ○ - centre points in cube, ■ - centre points in axial.



Fig. 2. Experimental Setup for ball end milling of Inconel 718-workpiece

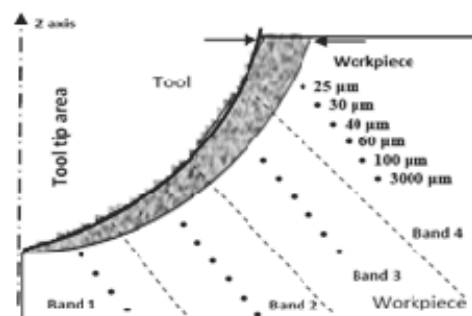


Fig. 3. Magnified view of the various band region

Table 1.  
Factors and their levels

| Sr. No | Machining parameters<br>(Symbol) (unit) unit)             | Parametric level |                  |                 |                |                   |
|--------|---|------------------|------------------|-----------------|----------------|-------------------|
|        |   | -1.5<br>(Lowest) | -1<br>(Lower)    | 0<br>(Centre)   | +1<br>(Higher) | +1.5<br>(Highest) |
| 1      | Spindle speed (V) (rpm)                                   | 1500             | 2000             | 3000            | 4000           | 4500              |
| 2      | Cutting feed (f) (mm/tooth)                               | 0.038            | 0.050            | 0.075           | 0.1            | 0.112             |
| 3      | Workpiece thickness (t) (mm)                              | 3.5              | 4                | 5               | 6              | 6.5               |
| 4      | Workpiece angle and tool path<br>orientation (d) (degree) | 45<br>Horizontal | 15<br>Horizontal | 0<br>Horizontal | 15<br>Vertical | 45<br>Vertical    |

A PVD coated TiAlN layered solid carbide end mill of 10 mm diameter was used for conducting ball end milling experiments. The insert has a specification helix angle 30 degree with ICT890 grade. A CNC Milling machine (Hardinge, Model -TM -2) was used for milling experiments (Fig. 2).

For the microhardness measurements, a cut surface of the machined sample was mounted in a Bakelite resin using hot mounting machine. Subsequently it was polished using metallurgical water proof SiC papers with grit 180 to 1500. These samples were further polished on cloth polishing machine to obtain fine mirror like surface. Microhardness testing was carried out using Vickers microhardness tester (Make-Shimatzu, Model-MV2). The experimental results in terms of microhardness beneath the machined surfaces are shown in Table 2.

### 3. Results and discussion

#### 3.1. Microhardness analysis

It is observed that the maximum hardness occurs at the region beneath 25  $\mu\text{m}$  to 100  $\mu\text{m}$  and it shows decreasing trend as the depth beneath the surface increases. The microhardness profile pattern shows significant variation from specimen to specimen as seen from Fig. 4. This is due to changes in the cutting parameters used for the milling experiments. It is observed that at large cutting speed as well as feeds, the thickness of work piece and workpiece inclination shows more hardness as compared to the other machining conditions (see Fig. 4. specimen #4, 5, 7, 17, 18). However, at lower cutting speed and feed, the work piece shows lower hardness value (see Fig. 4 specimen #23 and #24). The microhardness beneath the machined surface decreases as we go below the surface. The micro-hardness is higher very close to the machined surface (at 25 to 60  $\mu\text{m}$  depth) in all the bands. It is observed that the micro-hardness is higher near the machined surface layer and decreases with the depth of machined sub-surface due to a decrease in the work hardening of the material beneath the surface layer. In all the surface bands, the micro-hardness in band #1 and band # 2 appears to be the maximum followed by the band #3 and so on in all the experiments. The maximum micro-hardness value, i.e. 573.5 Hv is observed at band #1 in specimen # 4 (Fig. 4), which was due to higher mechanical loads produced on account of larger values of cutting speed and feed. On the other hand, the lowest micro-hardness value, i.e. 224.5 Hv is observed at band #4 in specimen # 25 (Fig. 4), which was performed at lower cutting speed and feed values within lined

workpiece. As the band #3 has relatively better surface finish, the various microhardness values in this region at different machining conditions are compared to other bands. Specimen #4 and #5 shows the microhardness similar or very near to the bulk microhardness for band 3 and 4 beneath 25  $\mu\text{m}$  in which the effect of mechanical workhardening is less significant. This softening that occurs on account specimen #5 band # 4. Further it is noticed that in band 3 and band 4 of specimen #24 and #25 that the microhardness profile is more over irregular from 25 to 300 micron beneath the machined surface.

#### 3.2. Statistical analysis of microhardness

##### Analysis of variance

The result of analysis of variance for the microhardness beneath the machined surface at 25 micron for band 3 is presented in Table 3. The value of "Prob. >F" for this model is higher than 0.05 (i.e.  $\alpha=0.05$ , or 95% confidence) indicates that the model is statistically insignificant.

None of the parameters shows statistically significant effects on the response variable which indicates that a stringent control is necessary to obtain the favourable microhardness values beneath the machined surface. It is seen that the model and the interaction terms show relatively better significance than linear and square terms. Table 4 shows the estimated regression coefficients for the quadratic model developed from the available microhardness data.

##### Analysis of means

In order to see the effect of input parameters on microhardness beneath the machined surface, main effects plots are derived using software. This plots show how the response variable vary with the changes in the corresponding input parameters.

Effect of Cutting Speed as far as the effect of cutting speed is concerned it is seen that the microhardness value is the highest at the lowest cutting speed at 54.95 m/min and drastically decreases up to 125.60 m/min. However it again shows some increment till 149 m/min. This behaviour can be explained as at lower cutting speed the tool contact length is more which causes higher frictional forces and therefore contribute to more mechanical load in the machining region and therefore the machined surface at 25 micron shows higher microhardness. As we increase the cutting speed the effect of temperature is significant leading to reduction in the mechanical load and thus causes reduction in the value of microhardness.

Table 2.  
Experimental observations for microhardness beneath machined surfaces

| Exp. No. | Input parameters |                  |                    |                       | Response variable Microhardness HV |        |        |        |
|----------|------------------|------------------|--------------------|-----------------------|------------------------------------|--------|--------|--------|
|          | Speed,(m/min)    | Feed, (mm/tooth) | w/p thickness,(mm) | wp angle and toolpath | Band 1                             | Band 2 | Band 3 | Band 4 |
| 1        | 78.5             | 0.05             | 4                  | 15 H                  | 231                                | 237    | 235    | 237    |
| 2        | 125.6            | 0.05             | 4                  | 15 H                  | 403                                | 462    | 463    | 364    |
| 3        | 78.5             | 0.1              | 4                  | 15 H                  | 266                                | 269    | 301    | 454    |
| 4        | 125.6            | 0.1              | 4                  | 15 H                  | 425                                | 408    | 307    | 312    |
| 5        | 78.5             | 0.05             | 6                  | 15 H                  | 236                                | 227    | 245    | 225    |
| 6        | 125.6            | 0.05             | 6                  | 15 H                  | 383                                | 304    | 280    | 245    |
| 7        | 78.5             | 0.1              | 6                  | 15 H                  | 377                                | 370    | 396    | 462    |
| 8        | 125.6            | 0.1              | 6                  | 15 H                  | 377                                | 337    | 340    | 347.5  |
| 9        | 78.5             | 0.05             | 4                  | 15 V                  | 219                                | 241    | 250    | 270    |
| 10       | 125.6            | 0.05             | 4                  | 15 V                  | 253                                | 381    | 357    | 377    |
| 11       | 78.5             | 0.1              | 4                  | 15 V                  | 374                                | 387    | 384    | 365    |
| 12       | 125.6            | 0.1              | 4                  | 15 V                  | 282                                | 285    | 255    | 237    |
| 13       | 78.5             | 0.05             | 6                  | 15 V                  | 411                                | 389    | 396    | 452    |
| 14       | 125.6            | 0.05             | 6                  | 15 V                  | 328.5                              | 362    | 380    | 402    |
| 15       | 78.5             | 0.1              | 6                  | 15 V                  | 365                                | 371.5  | 400    | 423    |
| 16       | 125.6            | 0.1              | 6                  | 15 V                  | 341                                | 369    | 396    | 407    |
| 17       | 94.2             | 0.075            | 5                  | 0H                    | 357                                | 471    | 367    | 336    |
| 18       | 47               | 0.075            | 5                  | 0H                    | 378                                | 480    | 491    | 503    |
| 19       | 157              | 0.075            | 5                  | 0H                    | 342                                | 333    | 396    | 346    |
| 20       | 94.2             | 0.025            | 5                  | 0H                    | 248                                | 242    | 293    | 330    |
| 21       | 94.2             | 0.12             | 5                  | 0H                    | 361                                | 404    | 440    | 320    |
| 22       | 94.2             | 0.075            | 3                  | 0H                    | 341                                | 365    | 364    | 362    |
| 23       | 94.2             | 0.075            | 7                  | 0H                    | 413.5                              | 407    | 423    | 427    |
| 24       | 94.2             | 0.075            | 5                  | 45V                   | 241                                | 232.5  | 247    | 221    |
| 25       | 94.2             | 0.075            | 5                  | 45H                   | 246                                | 211    | 250    | 243    |

Table 3.  
Analysis of variance for microhardness beneath the machined surface at 25 µm (band 3)

| Source         | DF | Seq SS | Adj MS | F    | P     |
|----------------|----|--------|--------|------|-------|
| Blocks         | 2  | 14584  | 7292   | 1.78 | 0.207 |
| Regression     | 14 | 64130  | 4581   | 1.12 | 0.422 |
| Linear         | 4  | 19798  | 4950   | 1.21 | 0.353 |
| Square         | 4  | 5333   | 1333   | 0.33 | 0.856 |
| Interaction    | 6  | 38999  | 6500   | 1.59 | 0.227 |
| Residual Error | 13 | 53208  | 4093   |      |       |
| lack-of-Fit    | 10 | 41635  | 4163   | 1.08 | 0.537 |
| Pure Error     | 3  | 11574  | 3858   |      |       |
| Total          | 29 | 131923 |        |      |       |

**Effect of feed**

It is observed that at the lowest feed of 0.025 mm/tooth, the microhardness is the highest and it decreases to the lowest value at the higher value of feed i.e. 0.125 mm/tooth. However there is no much variation in the microhardness between 0.050 to 0.100 mm/tooth. At the lowest feed, the length of contact remains engaged with the workpiece surface is more due to slower deformation rate. This causes more frictional forces generated during machining and hence increases the mechanically dominated plastic deformation of the surface. As a consequence the machined surface and subsurface shows higher microhardness.

**Effect of workpiece thickness**

It is seen from the plots that the thicker workpieces induce lower microhardness than the thinner one. It can be attributed to the fact that less rigidity of the workpiece tool combination during machining of thin workpieces produces larger forces and hence contributed to higher mechanical work hardening. On the other hand increased rigidity of the work-tool combination facilitates easy machining and the forces are less and thus show lower microhardness.

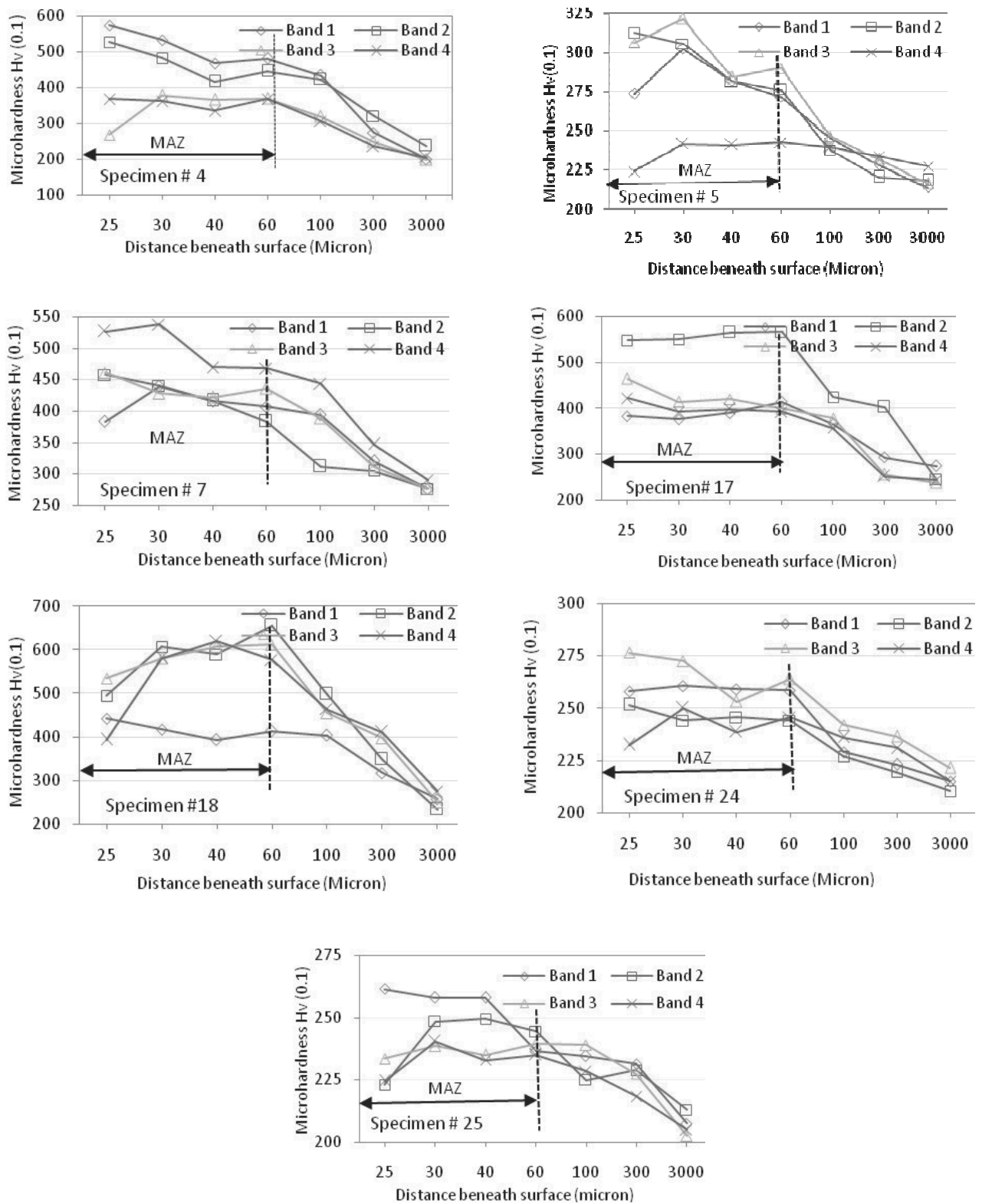


Fig. 4. Variation of microhardness below the machined surface in various band with MAZ

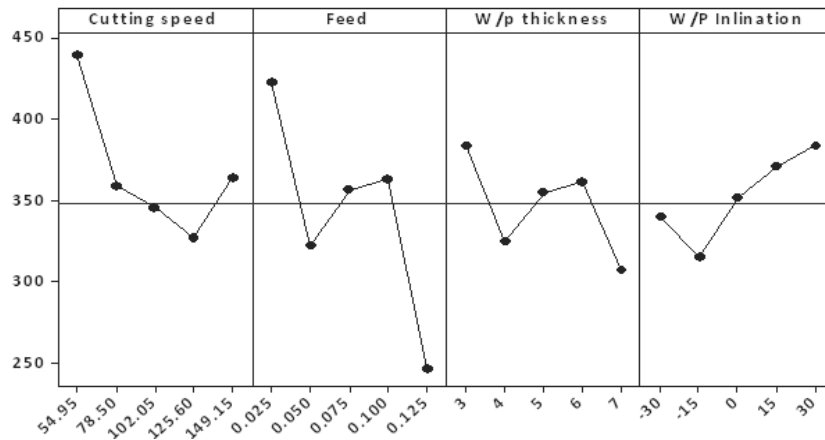
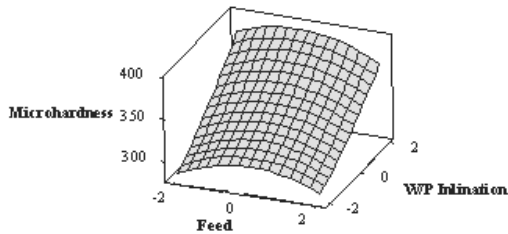
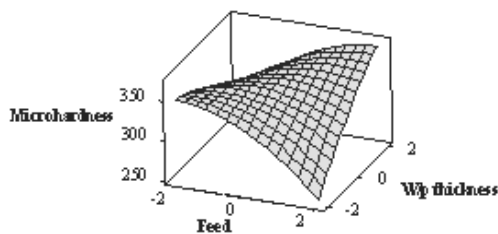


Fig. 5. Analysis of means for the microhardness beneath 25 micron for band 3

a) Surface Plot of Band 3 at 25 um vs W/P Inclination, Feed



b) Surface Plot of Band 3 at 25 um vs W/p thickness, Feed



c) Surface Plot of Band 3 at 25 um vs Feed, Cutting speed

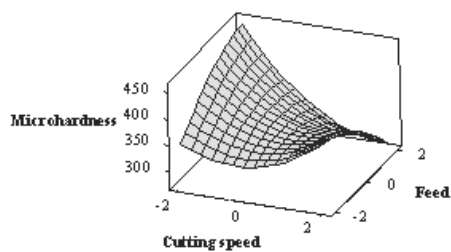


Fig. 6. Surface plot of band 3 at 25 micron

Table 4.

Estimated regression coefficients for band 3 at 25 um

| Term                            | Coef       |
|---------------------------------|------------|
| Constant                        | 838.672    |
| Block 1                         | -31.1000   |
| Block 2                         | 3.6000     |
| Cutting speed                   | -6.61860   |
| Feed                            | 1392.50    |
| W/p thickness                   | -74.3125   |
| W/P Inclination                 | -16.3319   |
| Cutting speed*Cutting speed     | 0.0208295  |
| Feed*Feed                       | -8316.67   |
| W/p thickness*W/p thickness     | -2.57292   |
| W/P Inclination*W/P Inclination | 0.00689815 |
| Cutting speed*Feed              | -24.5223   |
| Cutting speed*W/p thickness     | 0.697983   |
| Cutting speed*W/P Inclination   | 0.102442   |
| Feed*W/p thickness              | 462.500    |
| Feed*W/P Inclination            | -2.50000   |
| W/p thickness*W/P Inclination   | 1.51250    |

**Effect of workpiece inclination**

It is observed from the plots that when the work piece inclination was -15 degrees, the machined surface shows the lowest microhardness values. However it increases gradually when the workpiece inclination increases from 0 to 30 degrees with the horizontal. It is found that the larger inclination of workpiece causes generation of larger forces and hence contributed to more work hardening after machining and hence shows higher values of microhardness.

**Analysis of parameter interactions**

A combined effect of feed and workpiece inclination with tool orientation is presented in Fig. 6 (a) it is seen that the moderate

feed with 45° workpiece inclination shows higher values of microhardness as compared with either lower/higher feed combined with 15° horizontal workpiece inclination angle. Further the effect of feed combination with workpiece thickness is shown using response surface plot in Fig. 6(b). It is noticed that when microhardness the thicker workpiece are values machined at higher feed, the machined surface shows higher value of microhardness, however the thickness workpiece machined at lowest feed shows lower microhardness values of 25 micron beneath the machined surface.

## 4. Conclusions

A higher micro-hardness was obtained very close to the machined surface at 25 µm depth at a higher cutting speed, and higher axial feed. The microhardness variation was shown due to the thickness of workpiece and orientation of work piece. The statistical analysis of the experimental results show that the parameters contributing to volume of and rate of accumulation of the material ahead of cutting edge, i.e. depth of cut and feed rate, have significant influence on the magnitude of microhardness.

## Acknowledgements

Authors gratefully acknowledge the support provided by ARDB, Bangalore for the financial aid. Thanks are also due to assistance provided by Harshad Sonawane, for involvement of experimental setup.

## References

- [1] P. Lee, Y. Altintas, Prediction of ball end milling forces from orthogonal cutting data, *International Journal of Machine Tools and Manufactures* 36/9 (1996) 1059-1072.
- [2] Z.G. Wang, M. Rahman, Y.S. Wong, Tool wear characteristics of binder less CBN tools used in high-speed milling of titanium alloys, *Department of Mechanical Engineering* 258 (2005) 752-758.
- [3] M.C. Yoon, Y.G. Kim, Cutting dynamic force modeling of end milling operation, *Journal of Materials Processing Technology* 155-156 (2004) 1383-1389.
- [4] E.O. Ezugwu, Key improvements in the machining of difficult to cut aerospace superalloys, *International Journal of Machine Tools and Manufacture* 45 (2005) 1353-1367.
- [5] Z. Guimu, Y. Chao, S.R. Chen, A. Libao, Experimental study on the milling of thin parts of titanium alloy (TC4), *Journal of Materials Processing Technology* 138 (2003) 489-493.
- [6] K.D. Bouzakis, K. Efstathiou, A. Antoniadis, C. Charachaliou, P. Aichouh, Analytical experimental determination of surface roughness in milling, *Proceedings of the International Conference on Tribology „Balkan Trip 96”, Thessaloniki, 1996, 131-140.*
- [7] Y. Altintas, S. Engin, Generalized modeling of milling mechanics and dynamics: part II-inserted cutter, *Journal of Manufacturing Science and Engineering* 10 (1999).
- [8] Y. Altintas, S. Engin, Generalized modeling of milling mechanics and dynamics: part I-helical end mills, *Journal of Manufacturing Science and Engineering* 10 (1999).
- [9] A. Chen, W.C. Liu, N.A. Duffie, A surface topography model for automated surface finishing”, *International Journal of Machine Tools and Manufacture* 38 (1998) 543-550.
- [10] B. Montgomery, Y. Altintas, Mechanism of cutting force and surface generation in dynamic milling, *Journal of Engineering for Industry* 113 (1991) 160-168.
- [11] M. Alauddin, M.A. El Baradie, M.S.J. Hashmi, Optimization of surface finish in end milling inconel 718, *Journal of Material Processing and Technology* 56 (1996) 54-65.
- [12] A. Mansour, H. Abdalla, Surface roughness model for end milling: a semi-free cutting carbon case hardening steel (EN32) in dry condition, *Journal of Materials Processing Technology* 124 (2002) 183-191.
- [13] G.E.P. Box, N.R. Draper, *Response surfaces, mixtures, and ridge analyses*, Wiley, New Jersey, 2007.